THE ASTROPHYSICAL JOURNAL, 393:329–340, 1992 July 1

THE WOLF-RAYET SYSTEM WR 147: A BINARY RADIO SOURCE WITH THERMAL AND NONTHERMAL COMPONENTS

E. CHURCHWELL,[1] J. H. BIEGING,[2] K. A. VAN DER HUCHT,[3] P. M. WILLIAMS,[4]
T. A. TH. SPOELSTRA,[5] AND D. C. ABBOTT[6]

Received 1991 August 21; accepted 1992 January 9

ABSTRACT

A revised distance of 630 pc is derived for the Wolf-Rayet star WR 147(WN8) from newly obtained near-infrared photometry. This distance is almost free of reddening corrections, and it indicates that WR 147 is *not* associated with the Cyg OB2 association (which lies at a distance of 2 kpc), as previously thought. A terminal wind speed of 900 km s^{-1} is found for WR 147 from the P Cygni profile of the He I (2^1S–2^1P) line at 2.058 μm.

High-resolution VLA images were obtained at three different epochs at wavelengths 20, 6, 2, and 1.3 cm (although not all wavelength bands were imaged at each epoch) with angular resolutions of 1".60, 0".46, 0".14, and 0".11, respectively. These images show two radio components separated by 0".58 ($\sim$364 AU) in an approximately N–S direction. The optical astrometry of Moran et al. shows that the Wolf-Rayet star WR 147 coincides with the southern radio component WR 147S whose spectrum and visibility function are consistent with a thermal wind. The northern radio component WR 147N is clearly nonthermal. The radio emission from WR 147S can be accurately modeled by a spherical wind whose density decreases with distance as r^{-2}. We find an average mass-loss rate of $4.2 \pm 0.2 \times 10^{-5}\ M_\odot\ \mathrm{yr}^{-1}$ and a mean wind temperature of 9400 ± 1000 K.

Several mechanisms were investigated to determine if the observed X-ray luminosity could be produced by interaction of the wind from WR 147S with another star at the position of WR 147N. The only mechanism we found that could produce adequate X-ray luminosity is gravitational capture by a neutron star orbiting in a dense, slow, equatorial wind from WR 147S. This result lends support to the magnetic rotator model of Poe, Friend, & Cassinelli for W-R stars. We caution, however, that the X-ray emission could be produced by shocks in the wind of WR 147S or perhaps by colliding winds from WR 147S and WR 147N.

The flux density of the WR 147 system varies by as much as 50% at 21 cm over a period of a week or two and as much as 20% at 6 cm over a period of several weeks. The variations are probably associated with WR 147N.

Subject headings: binaries: visual — radio continuum: stars — stars: Wolf-Rayet

1. INTRODUCTION

Radio emission from a Wolf-Rayet (W-R) star was first detected toward γ^2 Vel by Seaquist (1976). Subsequently, about 40 W-R stars have been detected at radio wavelengths (see, for example, Florkowski & Gottesman 1977; Dickel, Habing, & Isaacman 1980; Hogg 1982; Felli & Panagia 1982; Bieging, Abbott, & Churchwell 1982; Abbott et al. 1986; Hogg 1989; and Moran et al. 1989). It was initially thought that stellar radio radiation was produced only by free-free emission in an ionized wind and that this emission could be used to determine accurate stellar mass loss rates. Abbott, Bieging, & Churchwell (1984) first suggested that not all the radio emission from massive stars is necessarily produced by a thermal wind. They showed that the two O stars 9 Sgr and Cyg OB2 No. 9 have unresolved, time-variable, nonthermal emission which might be produced by accretion onto an undetected compact companion. Abbott, Bieging, & Churchwell (1985) reported five additional nonthermal OB stellar radio emitters. Becker & White (1985a, b) found similar nonthermal emission from the W-R star HD 193793. Abbott et al. (1986) found that only 12% of a sample of 40 W-R stars within 3 kpc of the Sun are nonthermal emitters; this fraction is about half the percentage of nonthermal emitters among OB stars with luminosities greater than $10^6\ L_\odot$ located within 2.5 kpc of the Sun (Bieging, Abbot, & Churchwell 1989). White (1985) has proposed that nonthermal radio emission from massive stars (OB and W-R stars) originates in shocks which occur in the wind of a single star. Chen & White (1991) have also shown that X-ray emission can be produced via inverse Compton scattering of stellar UV photons by relativistic electrons produced in shocks embedded in the stellar wind. However, Williams et al. (1990) argue that the nonthermal radio and X-ray emission found in the eccentric WC7+O4 binary HD 193793 (WR 140 in the catalog of van der Hucht et al. 1981), which varies with orbital phase, is associated with the colliding winds of the WC and O-type components. Felli & Massi (1991) and Felli, Massi, & Cartarzi (1992) explain the varying nonthermal emission of θ^1 Ori A with the same binary model. Cohen et al. (1985) found evidence for colliding winds in the binary system MWC 349, although they did not explore the production of nonthermal radio emission in such a collision. Persi et al. (1990) find variable nonthermal radio emission from the luminous contact

[1] Washburn Observatory, University of Wisconsin-Madison, 475 North Charter Street, Madison, WI 53706
[2] Steward Observatory, University of Arizona, Tucson, AZ 85721
[3] SRON Space Research Utrecht, Sorbonnelaan 2, 3584 CA Utrecht, The Netherlands
[4] Royal Observatory Edinburgh, Blackford Hill, Edinburgh EH9 3HJ, Scotland, UK
[5] Netherlands Foundation for Research in Astronomy, P.O. Box 2, 7990 AA Dwingeloo, The Netherlands
[6] 1601 Mariposa, Boulder, CO 80302

binary Cyg OB2 No. 5. Thus both single and binary star models exist to explain nonthermal radio emission.

The Wolf-Rayet star WR 147 or AS 431 (in the catalog of Merrill & Burwell 1950) is a highly reddened WN8 star (Conti & Massey 1989). The properties of this star in the photometric system of Smith (1968) are $m_v = 14.89$ mag, $E(b-v) = 2.42$ mag, $A_v = 9.92$ mag, and $M_v = -6.7$ mag (Massey 1984; van der Hucht et al. 1988). Infrared emission from WR 147 has been reported by van der Hucht et al. (1985) and Stickland, Lloyd, & Willis (1985). Stickland et al. (1985) argued that WR 147 has *no excess* infrared emission and therefore no heated circumstellar dust; they also found $A_V = 12$ mag and $E(B-V) = 3.75$ mag, corresponding to $A_v = 13.32$ mag and $E(b-v) = 3.10$ mag in the system of van der Hucht et al. (1988). Assuming a bolometric correction $BC = -2.9$ (Schmutz 1990) and an absolute magnitude $M_V(\mathrm{WN8}) = -6.7$ (van der Hucht et al. 1988), we obtain a luminosity for WR 147 of $L = 5.5 \times 10^5\ L_\odot$.

Caillault et al. (1985) detected both radio and X-ray emission from WR 147; they found an X-ray flux $\geq 5 \times 10^{-12}$ ergs cm^{-2} s^{-1} (corresponding to a luminosity $\geq 0.5\ L_\odot$ based on a distance of 2 kpc) at energies 0.5–4.0 keV and a radio luminosity of $\sim 10^{20}$ ergs s^{-1} Hz^{-1}. Pollock (1987b) measured an X-ray luminosity about twice as large in the same band ($47 \pm 6 \times 10^{32}$ ergs s^{-1} for an assumed distance of 1900 pc), which, scaled to a distance of 630 pc (see below), becomes $0.13 \pm 0.02\ L_\odot$. The radio and X-ray emission were interpreted by Caillault et al. (1985) to arise in a chaotic stellar wind from a single, luminous W-R star; the mass loss rate inferred from the radio flux density was $\sim 3.9 \times 10^{-4}\ M_\odot$ yr^{-1} and the temperature of the X-ray emitting gas was found to be greater than 5.8×10^6 K. Moran et al. (1989) resolved WR 147 into two components separated by 0".6 at 6 cm using the MERLIN radio interferometer. Their synthesized beam was 0".15 × 0".13. The optical image of WR 147 coincides with the southern radio component WR 147S (Moran et al. 1989). Lortet et al. (1987) obtained speckle interferometry of WR 147 and found no companion with $\Delta m < 3$ mag within 1".5 of WR 147.

We report here both high-resolution radio images and results of a radio monitoring program of WR 147 which span the time interval 1984.3 to 1990.7. Our high-resolution images confirm that WR 147 is a binary radio source. We also confirm the suggestion of Moran et al. (1989) that WR 147N is a nonthermal emitter and WR 147S, which coincides with the W-R star, is a free-free source. The two components are connected by a bridge of radio emission. The star "system" is of particular interest because it is the first W-R star where one can clearly show that the thermal and nonthermal radio emission originate from distinctly different objects. For this star system, the standard model, in which the thermal and nonthermal emission originate in the wind of a single star, clearly does not apply. The discovery of this system provides a strong motivation to examine other possible mechanisms involving binary star systems. In the following, we give the data in § 2 and § 3, discuss results and explore possible mechanisms for producing the observed X-ray luminosity of the system in § 4, and summarize the main conclusions in § 5.

2. NEAR-INFRARED OBSERVATIONS

2.1. *The Distance to WR 147*

We observed WR 147 with the UKT6 photometer at the f/35 focus of the United Kingdom Infrared Telescope (UKIRT) located on Mauna Kea, Hawaii twice in 1983 and once in 1990. The L' filter is centered at 3.8 μm. The results are given in Table 1. The differences are slightly greater than we would expect from the standard transfers, but not great enough to be certain that the star is variable at these wavelengths.

TABLE 1

NEAR-INFRARED PHOTOMETRY OF WR 147

Date	Band H (mag)	K (mag)	L' (mag)
1983 Jul 12	4.90	4.17	3.28
1983 Aug 1	4.90	4.18	3.24
1990 Aug 28	4.88	4.11	3.19

Determination of the distance to WR 147 from its visual distance modulus is strongly dependent on its uncertain reddening, which is partly a consequence of its having unusual colors in the visible: $b-v$ is too blue for its $v-r$ color. The effects of this can be alleviated by working in the infrared in the H, K, and L' bands where the reddening is only a fraction of that in the visible. The flux from W-R stars in the near-infrared is a combination of photospheric and stellar wind emission, with the latter dominating at the longer wavelength. There is no a priori reason why the dispersion in the photospheric luminosities of W-R stars of a given subtype should be any greater or less than the dispersion in the stellar wind luminosities, so it is valuable to consider both. We have, therefore, estimated the absolute H, K, and L' magnitude of WR 147 by comparison with the only known galactic WN8 star in an association, which is WR 105 in Sgr OB1 (Lundstrom & Stenholm 1989). Its infrared photometry is given in Table 2 from observations made at UKIRT and ESO (van der Hucht, Williams, & Yudiawati, in preparation). The near-infrared photometric systems at the two observatories are very similar. The absolute H, K, and L' magnitudes derived for WR 105 are also given in Table 2, dereddened according to $A_v = 8.65$ mag and adopting 1.58 kpc for its distance.

To determine the distance and reddening of WR 147, we iterated as follows. Dereddening the observed HKL' magnitudes of WR 147 according to the narrow-band visual extinction $A_v = 9.92$ mag (van der Hucht et al. 1988) and adopting the absolute magnitudes derived from WR 105, we derive a mean IR distance modulus of 9.26 mag for WR 147. This can be reconciled with the absolute visual magnitude of the WN8 subtype (-6.7, van der Hucht et al. 1988) if the extinction is $A_v = 12.3$. This is equivalent to $A_V = 11.2$ and is closer to the value found by Stickland et al. (1985) from fitting the $UBVR$,

TABLE 2

OBSERVED, DEREDDENED, AND ABSOLUTE IR MAGNITUDES OF WR 105

Date	H (mag)	K (mag)	L' (mag)	Observatory
1983 Jul 13	6.33	5.78	5.09	UKIRT
1988 Apr 8	6.32	5.78	5.06	ESO
1988 Apr 10	6.31	5.84	5.12	UKIRT
1991 Apr 2	6.30	5.71	5.01	ESO
Dereddened	5.09	5.04	4.68	
Absolute	−5.91	−5.96	−6.32	

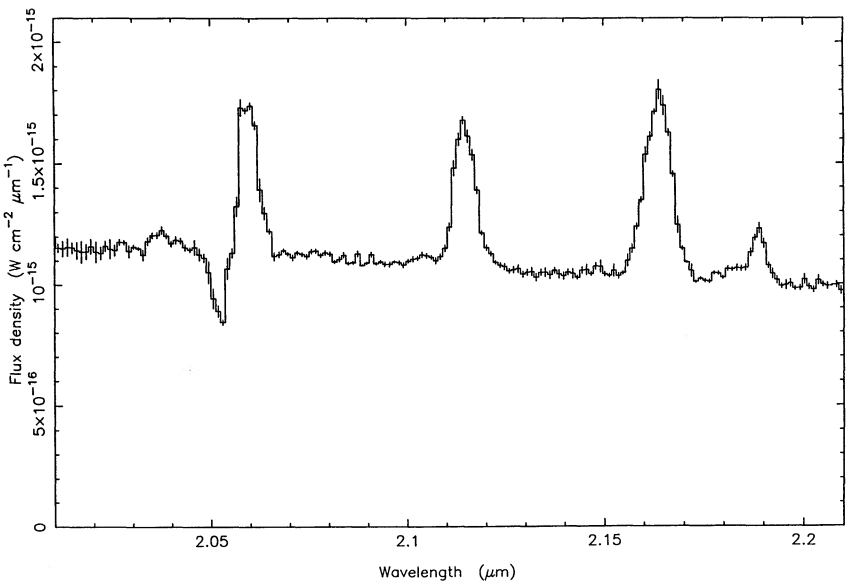

FIG. 1.—A 2 μm spectrum toward WR 147 (=AS 431) obtained with the CGS2 spectrometer on the UKIRT telescope on 1990 June 23. The resolution is 1.67×10^{-3} (500 km s^{-1}). The features, in order of increasing wavelength, are He II (15–8) at 2.037 μm; He I (2^1S–2^1P) at 2.058 μm; He I (4*s*–3*p* singlet and triplet) at 2.113 μm; H + He I (7–4) at 2.165 μm; and He II (10–7) at 2.189 μm. The blue edge of the P Cygni profile of He I (2^1S–2^1P) line implies a wind terminal velocity of 900 km s^{-1}.

bvr, and infrared photometry to a blackbody. Using our higher estimate of extinction, we derived new IR distance moduli, giving a mean of 9.03 mag. We used this to refine the visual extinction and hence IR extinctions and distance moduli, yielding a mean distance modulus of 9.01 mag. The corresponding visual extinction is $A_v = 12.58$ or $A_V = 11.5$. Even if the adopted value of the extinction is wrong by 2 mag, the change in distance modulus from *HKL'* photometry is only 0.2 mag. We adopt a distance of 630 pc. The formal error due to photometric uncertainties is ±70 pc; however, the error introduced by the assumption that WR 147 and WR 105 have identical luminosities is probably larger (perhaps as much as 1 mag in the distance modulus). A distance of 630 pc would make WR 147 the second nearest W-R star after the WC8+O8 γ^2 Vel system at 450 pc.

WR 147 is apparently about 3 times closer to us than the Cyg OB 2 association and cannot be a member of this system as previously assumed. Two important consequences of the reduced distance are that the X-ray luminosity of WR 147 is reduced to about 0.13 $L_\odot$ and its mass loss rate (as we show below) is reduced to a value consistent with other W-R stars. Also, apparently much of the extinction seen toward the Cyg OB2 association occurs much closer to us (<630 pc) than the molecular cloud with which Cyg OB2 is associated or it is local to WR 147 without being close enough to be heated by the stellar radiation.

2.2. *The Terminal Wind Velocity of WR 147*

We measured the terminal wind velocity of WR 147S from the absorption component of the 2.058 μm He I (2^1S–2^1P) line following Williams & Eenens (1989). A 2 μm spectrum was observed at our request with the CGS2 spectrometer on the UKIRT on 1990 June 23. The 637 line mm^{-1} grating was used in the first order giving a spectral resolution of 500 km s^{-1} (FWHM). The He I line is close to atmospheric CO_2 features which were corrected for by observation of a standard star at the same elevation as WR 147. These features also provided a check on the wavelength calibration.

The spectrum is shown in Figure 1. It resembles that of the WN8 star HD 96548 observed by Hillier (1985). The strong He I (2^1S–2^1P) line has a P Cygni profile. In this case, the violet edge of the absorption corresponds to a terminal velocity of 900 km s^{-1}. This value is close to the terminal velocities found for other WN8 stars by Prinja, Barlow, & Howarth (1990) from *IUE* observations. The other strong lines are He I (4*s*–3*p*: singlet and triplet) at 2.113 μm, H + He I (7–4) at 2.165 μm, and He II (10–7) at 2.189 μm. He II (15–8) is also visible at 2.037 μm. The weakness of He II (10–7) supports the reclassification from WN7 to WN8 by Conti & Massey (1989).

3. RADIO OBSERVATIONS

3.1. *The VLA Data*

Three sets of images at wavelengths ranging from 20 cm to 1.3 cm were obtained with the Very Large Array (VLA) operated by NRAO[7] in the A-configuration during the latter part of 1984 and early 1985. Angular resolutions ranged from ~1.″6 to ~0.″1 at wavelengths from 21 cm to 1.3 cm, respectively. The dates of observation, synthesized half-power beam width (HPBW), rms noise in the image, source position, maximum and minimum angular diameters θ_s and ϕ_s (deconvolved from the synthesized beam), and the integrated flux density determined from a Gaussian fit and from a simple integration over the area occupied by the source are given in Table 3 at each frequency ν. The data were all reduced using precisely the same techniques. The flux densities are on the Baars et al. (1977) scale. At 1.46 GHz (21 cm), the resolution is too low to reveal that WR 147 is a double source. At 5 GHz (6 cm), the double

[7] The National Radio Astronomy Observatory is operated by Associated Universities, Inc., under cooperative agreement with the National Science Foundation.

TABLE 3

VLA OBSERVATIONS OF WR 147

Epoch	Frequency (GHz)	Synthesized HPBW	rms Noise (mJy)	Component	R.A. (1950) 20^h34^m	Decl. (1950) 40°10′	θ_s max[a]	ϕ_s min[a]	P.A. (°)	Integrated Gauss[b] (mJy)	Flux IMEAN (mJy)	Peak T_B (K)
1984 Nov 27.....	1.45	1.″60	0.112	All	53.841	38.″05	1.″12	0.″83	170	26.1	26.1	4050
	4.80	0.46	0.122	S	53.848	37.59	0.46	0.33	164	21.4		2975
				N	53.838	38.22	0.58	0.23	92	11.9		1600
				Total							38.6	
	15.0	0.14	0.284	S	53.850	37.58	0.18	0.16	98	36.9	42.4	4430
				N	53.835	38.13	0.35	0.26	176	9.3	7.6	495
				Total							50.0	
1985 Jan 13.....	15.0	0.16	0.570	S	53.849	37.59	0.17	0.14	18	38.7	41.4	4360
				N	53.838	38.11	0.23	0.13	97	7.9	7.9	710
				Total							49.3	
	22.5	0.11	1.150	S	53.849	37.58	0.14	0.11	76	49.4		4730
				N	...	...	...	...			<3.5[c]	<740
				Total							59.1	
1985 Feb 16	4.8	0.47	0.113	S	53.848	37.59	0.41	0.31	162	19.4		2830
				N	53.840	38.20	0.52	0.29	99	13.3		1760
				Total							36.5	
	15.0	0.14	0.138	S	53.847	37.57	0.15	0.13	68	31.3	35.5	4500
				N	53.837	38.10	0.27	0.15	77	6.0	7.4	550
				Total							42.9	

[a] These are maximum and minimum deconvolved source half-power widths (FWHM). IMFIT in AIPS was applied to determine these values. P.A. is the position angle of the major axis of the source.

[b] This is the integrated flux density for the fitted Gaussian component. The IMEAN result is the simple integral over the area occupied by the source.

[c] 3 σ upper limit.

component structure of WR 147 is apparent but the components are not well enough resolved for us to derive separate parameters for them reliably. Nevertheless, the Gaussian fit results are close to those measured by Moran et al. (1989). At $\lambda \leq 2$ cm, the northern and southern components are well separated and in Table 3 observed parameters for the separate components are given. Peak brightness temperatures are given in the last column of Table 3. The values for WR 147S are consistent with the derived wind temperatures and a source which is optically thick only in the inner core but thin farther out. For WR 147N, the peak T_B values are rather low, probably indicating either an optically thin source and/or a low filling factor in the synthesized beam. The 5–15 GHz spectral indices from the Gaussian fits were -0.4 ± 0.1(N) and $+0.6 \pm 0.1$(S) on 1984 November 27 and -0.5 ± 0.1(N) and $+0.5 \pm 0.1$(S) on 1985 February 16. Between 15 and 22.5 GHz on 1985 January 13 the spectral indices were $+0.9 \pm 0.3$(S) and < -2(N). The observed images at each epoch are shown in Figures 2–4. These images show quite clearly that WR 147 is a double radio source. Further, the sources are connected by a bridge of radio continuum emission at 2 cm. This bridge is well resolved at $\lambda \leq 2$ cm; it is not an artifact of poor resolution.

The 2 cm images obtained on 1984 November 27 and 1985 February 16, and the 6 cm image of Moran et al. (1989) all show low brightness extensions on approximately opposite sides of WR 147S which appear to be approximately aligned with the two radio components. Although the images differ somewhat at the lowest brightness contours, the fact that three entirely independent images show extensions almost along the same general direction suggests that these extensions are real, and not image artifacts.

On 1985 January 13 only 15.0 and 22.5 GHz images were obtained. At 22.5 GHz, only WR 147S was detected. If we assume that the flux density at 22.5 GHz is produced entirely by a thermal wind from WR 147S, then we can extrapolate its flux density to other frequencies by assuming the standard spectral index of 0.6. The extrapolated flux density at 15.0 GHz (46.3 ± 3.5 mJy) is in good agreement with the observed flux densities of WR 147S (see Table 3). At lower frequencies, the extrapolated flux densities are systematically lower than the observed values because WR 147N contributes significant flux below 15.0 GHz. This comparison suggests that WR 147S has a radio spectrum consistent with a thermal wind, but WR 147N is nonthermal. This suggestion is confirmed by the visibility analysis discussed below in § 4.1 and illustrated in Figure 6.

3.2. *The WSRT Data*

A functional description of the Westerbork Synthesis Radio Telescope (WSRT) is given by Baars et al. (1973) and Bos, Raimond, & Van Someren Greve (1981). The WSRT observations were obtained at wavelengths of 21 and 6 cm. The shape and size of the synthesized beam (i.e., $12'' \times 12''$ cosec (δ) and $3.''5 \times 3.''5$ cosec (δ) for 21 and 6 cm, respectively, where δ is the declination) depend on the distribution of the projected baselines included in the maps. This is different for any observation shorter than 12 hr and with missing baselines. The flux densities are on the Baars et al. (1977) scale.

In Table 4, we summarize high-resolution continuum flux density measurements of WR 147 at 21 and 6 cm during the period 1988.5–1990.7. The errors are the rms noise levels in each image. None of the WSRT data have high enough resolution to detect the double structure of WR 147, but they do provide a valuable record of the radio flux density of the entire system over a significant period of time. A 12 hr synthesis image was obtained with the WSRT on 1989.975 at 21 cm; this image shows that the region around WR 147 is remarkably free of confusing radio sources. There are no point sources above ~ 0.5 mJy within a radius of $\sim 5'$. This considerably

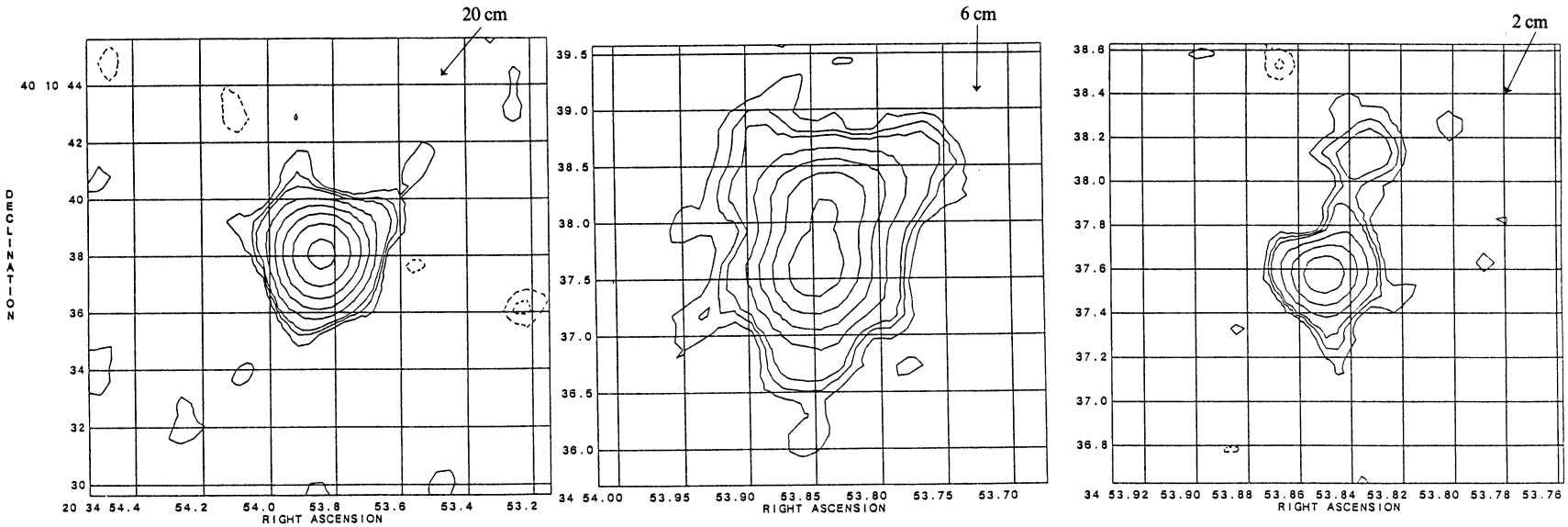

FIG. 2.—The VLA images obtained on 1984 November 27 at 20 cm, 6 cm, and 2 cm with angular resolutions of 1.″60, 0.″46, and 0.″14, respectively. The field of view decreases from left to right; note the coordinates. At 6 cm it is already clear that the source is double, and at 2 cm the components are resolved. Note the bridge of emission between the two components at 2 cm. At 20 cm the peak flux = 1.8080×10^{-2} Jy beam^{-1}; levels = 1.1200×10^{-4} Jy beam^{-1} times (−4.00, −3.00, −2.00, 2.000, 3.000, 4.000, 8.000, 16.00, 32.00, 64.00, 128.00). At 6 cm the peak flux = 1.2696×10^{-2} Jy beam^{-1}; levels = 1.2000×10^{-4} Jy beam^{-1} times (−4.00, −3.00, −2.00, 2.000, 3.000, 4.000, 8.000, 16.00, 32.00, 64.00, 128.00). At 2 cm the peak flux = 1.6469×10^{-2} Jy beam^{-1}; levels = 3.0000×10^{-4} Jy beams^{-1} times (−4.00, −3.00, −2.00, 2.000, 3.000, 4.000, 8.000, 16.00, 32.00, 64.00, 128.00).

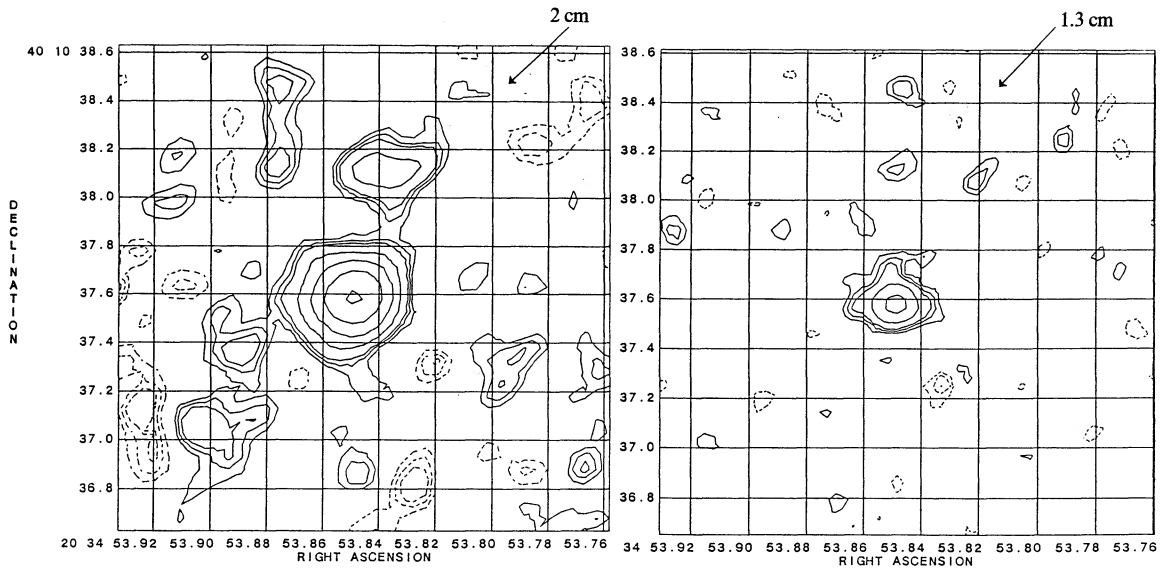

FIG. 3.—The VLA images obtained on 1985 February 16 at 6 cm and 2 cm with angular resolutions of 0".46 and 0".14, respectively. Note the bridge between the two components at 2 cm. At 2 cm the peak flux = 2.0902×10^{-2} Jy beam^{-1}; levels = 3.0000×10^{-4} Jy beam^{-1} times (−4.00, −3.00, −2.00, 2.000, 3.000, 4.000, 8.000, 16.00, 32.00, 64.00, 128.00). At 1.3 cm the peak flux = 2.2498×10^{-2} Jy beam^{-1}; levels = 1.1500×10^{-3} Jy beam^{-1} times (−4.00, −3.00, −2.00, 2.000, 3.000, 4.000, 8.000, 16.00, 32.00, 64.00, 128.00).

simplifies the imaging and flux density measurements of WR 147.

In Figure 5 we have plotted the measured flux densities at 6 and 21 cm of the WR 147 system (sum of both radio components) as a function of time. The data plotted in Figure 5 show that flux density variations as large as 50% at 21 cm and 20% at 6 cm have been observed. Although the errors at 21 cm are largest during the period of maximum fluctuation, the error bars of the extrema do not overlap by a reasonably large margin. We conclude that the flux-density variations cannot be due to observational error, but must indicate intrinsic variations in the WR 147 system. Unfortunately, the 6 and 21 cm measurements were not obtained simultaneously so we do not know whether the flux densities change by the same amount and in the same sense at both frequencies. Nor can we say with certainty that the flux density at 6 cm is always greater than that at 21 cm. Nonetheless, it appears that the 21 cm flux densities have significantly larger variations than at 6 cm, and the 21 cm flux densities appear to be generally (if not always) less than those at 6 cm during the periods for which we have observations. There is no obvious period of variation at either wavelength, but we stress that the intervals of time over which measurements have been made are small and the sampling within these periods has not been systematic. The sampling

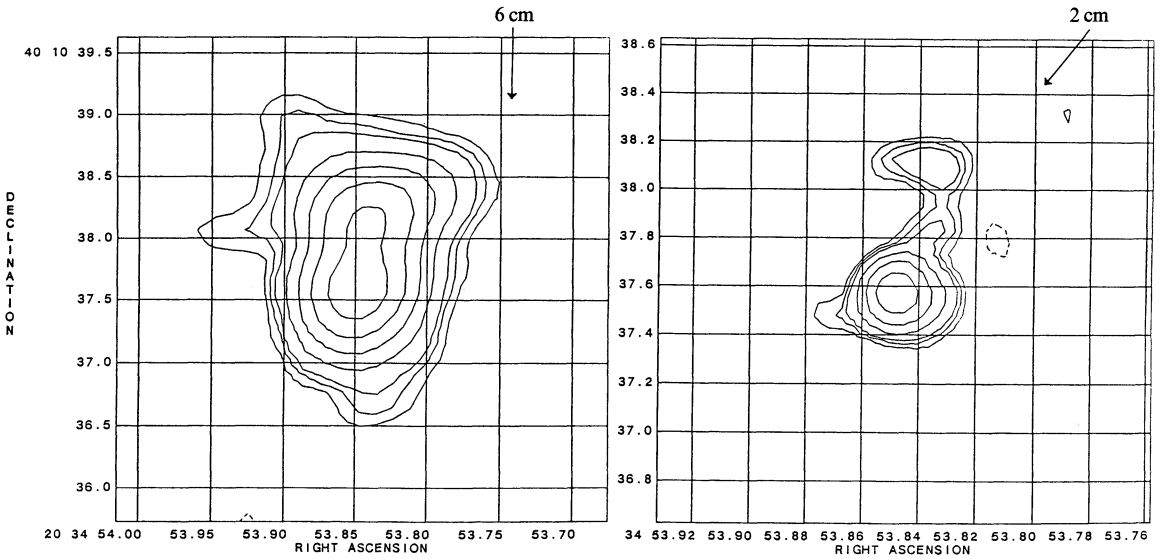

FIG. 4.—The VLA images obtained on 1985 February 16 at 6 cm and 2 cm with angular resolution of 0".46 and 0".14, respectively. Note the bridge between the two components at 2 cm. At 6 cm the peak flux = 1.2517×10^{-2} Jy beam^{-1}; levels = 1.2000×10^{-4} Jy beam^{-1} times (−4.00, −3.00, −2.00, 2.000, 3.000, 4.000, 8.000, 16.00, 32.00, 64.00, 128.00). At 2 cm the peak flux = 1.6467×10^{-2} Jy beam^{-1}; levels = 3.0000×10^{-4} Jy beam^{-1} times (−4.00, −3.00, −2.00, 2.000, 3.000, 4.000, 8.000, 16.00, 32.00, 64.00, 128.00).

TABLE 4

WSRT FLUX DENSITY MEASUREMENTS OF WR 147

Date	S(6 cm) (mJy)	S(21 cm) (mJy)
1988.54.....	32.62 ± 0.24	
1988.93.....	...	13.00 ± 0.65
1989.03.....	...	16.89 ± 1.10
1989.07.....	...	15.82 ± 1.20
1989.564.....	36.00 ± 0.54	
1989.608.....	37.55 ± 0.46	
1989.616.....	36.45 ± 0.54	
1989.646.....	37.13 ± 0.53	
1989.712.....	35.99 ± 0.59	
1989.764.....	34.45 ± 0.62	
1989.794.....	...	30.78 ± 2.70
1989.808.....	...	30.98 ± 1.32
1989.824.....	...	22.57 ± 2.30
1989.879.....	...	33.86 ± 1.57
1989.898.....	...	26.71 ± 0.95
1989.917.....	...	28.57 ± 0.70
1989.939.....	...	28.77 ± 0.79
1989.961.....	...	29.30 ± 0.93
1989.975.....	...	32.12 ± 0.69
1989.994.....	...	23.22 ± 1.15
1990.008.....	...	27.11 ± 1.04
1990.033.....	...	29.23 ± 1.69
1990.057.....	...	28.32 ± 0.68
1990.353.....	35.69 ± 0.50	
1990.370.....	33.40 ± 0.59	
1990.400.....	30.63 ± 0.37	
1990.454.....	35.40 ± 0.45	
1990.501.....	...	29.03 ± 0.79
1990.539.....	...	28.40 ± 0.55
1990.559.....	...	26.92 ± 0.61
1990.586.....	...	24.84 ± 0.44
1990.632.....	...	26.57 ± 0.46
1990.654.....	...	23.80 ± 0.61
1990.684.....	...	27.89 ± 0.50

interval was, unfortunately, too long to place any meaningful limits on the source size. The shortest interval between samples is about 5–6 days; variations of 25%–30% are detected at 21 cm in this period.

4. RESULTS

4.1. *Wind Properties*

4.1.1. *Standard Radiation Driven, Spherical Wind Analysis*

In this section, we will assume that the wind from the Wolf-Rayet star is responsible for the free-free emission from WR 147S. We will use the distribution of thermal radio visibilities with baseline (in the manner of Becker & White 1985a, b) to determine the mass loss rate $\dot{M}$ and the mean temperature of the wind. To do this, it is necessary to separate the emission of WR 147S from the rest of the source. At 15 GHz, the two sources are well separated (see Figs. 2–4). We, therefore, constructed a clean-component model for the northern source by "cleaning" only a small box containing just WR 147N. The AIPS task UVSUB was used to subtract the WR 147N clean components from the visibility data. *Annular-averaged* amplitudes and phases were constructed from the visibility data with WR 147N visibilities removed. The annular-averaged amplitudes were then used to model the wind emission to determine the best-fit wind temperature and mass loss rate. Only the 15 and 22.5 GHz data were used for this purpose. We assume a distance of 630 pc, a wind terminal velocity of 900 km s^{-1}, and a spectral type WN8. We adopt for a WN8 star a mean atomic weight per ion $\mu = 2.70$ (Willis 1991), a net charge per ion of unity (i.e., $Z = 1$), and unity for the mean number of electrons per ion (i.e., $\gamma = 1$). The values of μ, Z, and γ are uncertain for W-R stars, particularly at distances greater than $100R_*$ from the central star where the radio emission is produced. Uncertainties in the abundances, ionization structure of the wind, and distance (D) produce uncertainties in the derived mass loss rate since $\dot{M} \propto \mu D^{3/2}/Z(\gamma)^{1/2}$. We assume that the wind is spherically symmetric at $r > 100R_*$, has a constant temperature (i.e., we do not attempt to account for temperature gradients), and density decreases with distance as $\rho(r) \propto r^{-2}$ (i.e., a constant velocity wind). With these assumptions, models of the wind were constructed by adjusting the temperature and mass loss rate $\dot{M}$ such that the annular-averaged amplitudes predicted by the model were in good agreement with the aver-

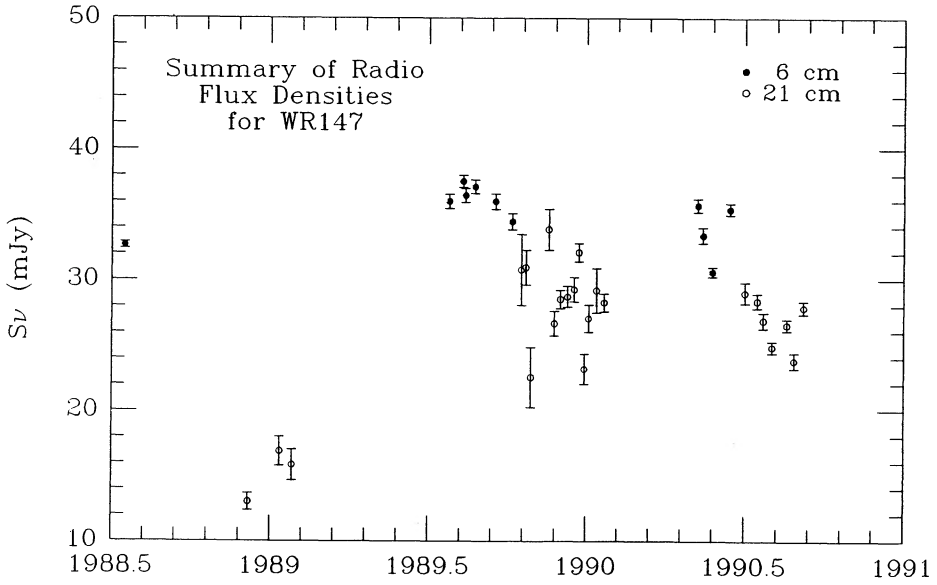

FIG. 5.—The flux densities measured with the WSRT at 6 cm and 21 cm are plotted as a function of time. One sees that the 6 cm flux densities are larger than at 21 cm and the source varies by as much as 50% at 21 cm over a period of a week or so and as much as 20% at 6 cm over a period of several weeks. The fact that the variations are larger at 21 cm than at 6 cm supports the supposition that the nonthermal radio component gives rise to the variable emission.

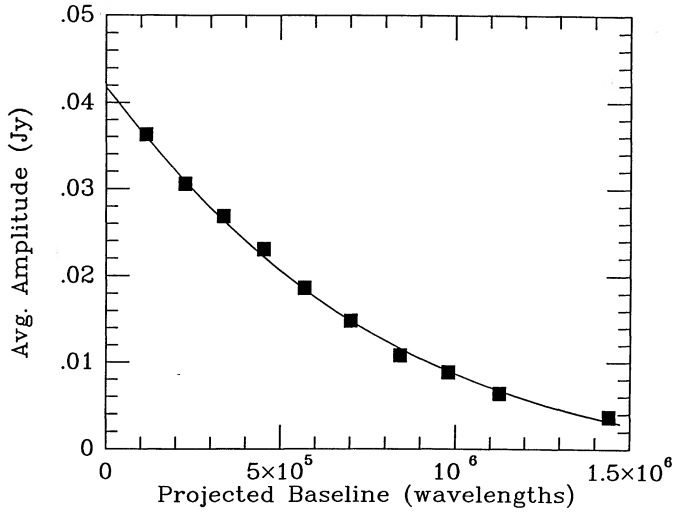

FIG. 6.—The annular-averaged amplitudes of the 15 GHz visibilities obtained on 1985 February 16 are plotted as a function of projected baseline. The observations are indicated by the filled squares. The size of the symbols is approximately 2 σ in the amplitudes of the annular averages. The curve is a theoretical fit to the observations achieved by adjusting the mass loss rate and the wind temperature to minimize χ^2.

aged values at 15 GHz for each epoch. The "best-fit" model for the 1984 November 27 data predicts $T = 8400 \pm 2000$ K and $\dot{M} = 4.3 \pm 0.3 \times 10^5\ M_\odot\ \mathrm{yr}^{-1}$; for 1985 January 13 it predicts $T = 10{,}000 \pm 3000$ K and $\dot{M} = 4.3 \pm 0.6 \times 10^{-5}\ M_\odot\ \mathrm{yr}^{-1}$; and for 1985 February 16, we find $T = 9800 \pm 2000$ K and $\dot{M} = 4.0 \pm 0.2 \times 10^{-5}\ M_\odot\ \mathrm{yr}^{-1}$. A similar analysis of the 22.5 GHz visibilities obtained on 1985 January 13 gave $T = 12{,}000$ (+10,000, −5000) K and $\dot{M} = 3.9 \pm 0.5 \times 10^{-5}\ M_\odot\ \mathrm{yr}^{-1}$. Since the 22.5 GHz data had a lower signal-to-noise ratio than the 15 GHz data, the errors are larger but the values are in agreement within the errors with the results from the 15 GHz data. The average wind parameters for these three epochs are $T = 9400 \pm 1000$ K and $\dot{M} = 4.2 \pm 0.2 \times 10^{-5}\ M_\odot\ \mathrm{yr}^{-1}$, where the estimated errors are large enough to include the range of values derived at each epoch. In Figure 6, we show the observed and predicted 15 GHz annular-averaged amplitudes versus baseline for the 1985 February 16 data. The symbols represent the observations and the continuous curve the predictions of the "best-fit" model. The best fit was obtained by minimizing χ^2 for the models. Figure 6 illustrates that spherically symmetric, single-temperature wind models fit the observations quite well. If deviations from spherical symmetry and/or temperature gradients were present in the wind, we would be unlikely to detect them because the azimuthal averaging of our data tends to average out these effects. The mass loss rate found here for WR 147 is very close to the mean value for W-R stars [about $5 \times 10^{-5}\ M_\odot\ \mathrm{yr}^{-1}$, according to Prinja et al. (1990) and Willis (1991)].

4.1.2. *Magnetic Rotator Analysis*

It has been known for sometime that the winds of W-R stars carry several times more momentum than that in their radiation fields. Specifically, for WR 147, we find $\eta = \dot{M}v_\infty/(L_*/c) \sim 3.3$ using the mass loss rate found above and the luminosity given in § 1. The rate of momentum transported in the winds ($\dot{M}v_\infty$) of W-R stars relative to that carried by their radiation fields (L_*/c) typically lies in the range $1 \leq \eta \leq 30$ according to Willis (1991). These large values of η have brought the theory of radiation-driven winds, which seems to work well for O stars, into serious question for W-R stars. As a consequence, alternative models have been proposed. One that appears particularly promising is the "magnetic rotator" model introduced by Poe, Friend, & Cassinelli (1989) for W-R stars. Zickgraf et al. (1985) proposed an equatorial wind driven by rotation for B[e] stars, but the possible role of magnetic fields was not considered. This model has been developed further for Be stars by Waters et al. (1988). Cassinelli (1990, 1991) has given good summaries of the magnetic rotator theory and its limitations. In this model, W-R stars have a high-velocity, highly ionized, radiatively driven *polar* wind and a slower, denser, lower ionization, *equatorial* wind controlled by rotational and magnetic forces. The equatorial wind is primarily responsible for the observed radio emission and the polar wind is detected by UV resonance lines of Si IV, C IV, and N V. In this model, the measured wind speed is a function of both orientation of the polar flow and the equatorial mass loss disk to the line of sight and of the observational probe used. The fact that the terminal velocity implied by the He I 2.058 μm line is about the same as those found for other WN8 stars from high-ionization species such as C IV, Si IV, and N V by Prinja et al. (1990) suggests that the He I 2.058 μm line is produced in the polar flow (if a two-component wind model applies) rather than the equatorial wind. If a "magnetic rotator" model is assumed for WR 147S, how will its mass loss rate be modified? To answer this question, we used an extended version of the $\dot{M}$–v_∞ plot (Fig. 5) in Poe et al. (1989) to form an "iso-radio flux" curve that passes through an equatorial mass loss rate of $4.2 \times 10^5\ M_\odot\ \mathrm{yr}^{-1}$ at a terminal velocity of 900 km s^{-1} and is parallel to the "iso-radio flux" curve shown in the original figure. In this model, the equatorial mass loss rate for arbitrary equatorial out-flow velocity v_e is related to the mass loss rate determined from the radio flux density assuming a spherical wind with terminal velocity $v_\infty = 900$ km s^{-1}

$$\dot{M}(v_e) = \frac{\dot{M}(v_\infty)}{v_\infty} v_e = 4.67 \times 10^{-8} v_e\ ,$$

where $\dot{M}$ (v_e) is in $M_\odot\ \mathrm{yr}^{-1}$, $\dot{M}(v_\infty) = 4.2 \times 10^{-5}\ M_\odot\ \mathrm{yr}^{-1}$, and v_e is in km s^{-1}. Thus, $\dot{M}(v_e) \propto (v_e)$ and the density and mass flux in the equatorial wind depend on v_e.

Although we have not analyzed in detail the effect on our temperature analysis when an equatorial mass loss disk is viewed face-on, we suspect that our analysis is probably still valid. If the disk is assumed to flare out at a fixed opening angle with radius and $\rho(r) \propto r^{-2}$ in the disk, then the line-of-sight distance through the disk is proportional to r. Thus, the emission measure falls off as r^{-3}, just as in the case of a uniform spherical wind. The temperature is determined from the visibility function, which depends on the brightness distribution in both cases. The correction from the spherical case will depend on the exact disk geometry. Schmid-Burgk (1982) considered conical winds and equatorial belts and found that the corrections depend on geometry and viewing angle, but that they are not very large except for very narrow jets or thin disks. Reynolds (1986) considered collimated jets, which are not relevant to an equatorial disk. Neither Schmidt-Burgk nor Reynolds considered the temperature derived from visibility functions.

4.2. *The Spectral Indices*

Since the WR 147 system is a variable radio source, determination of the flux density distributions of each radio com-

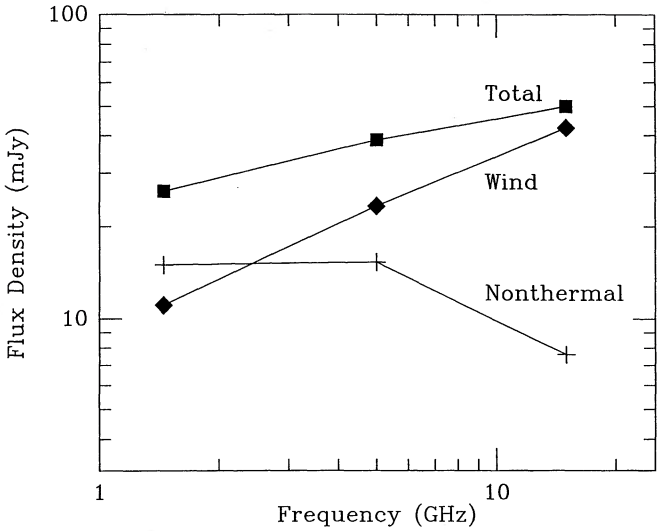

FIG. 7.—The spectrum of the WR 147 system (northern plus southern components) is shown as filled squares. The flux densities of the thermal wind associated with the W-R star, based on the mass loss rate and wind temperature derived from the best-fit models of the visibilities are shown as filled diamonds. The data are from 1984 November 27. The residuals (total minus the wind flux densities) are shown as plus symbols and are labeled nonthermal because they represent the flux densities of the northern nonthermal radio component.

ponent separately can only be done using observations taken essentially simultaneously. During 1984 February 27, flux densities were obtained at 21, 6, and 2 cm. In Figure 7, the observed total flux densities of the system (using IMEAN) for this data are plotted as filled squares. Based on the discussion above, we assume that WR 147S is due entirely to a thermal wind. Using the wind temperature and mass loss rate given above for this date, the flux densities of the wind were calculated for 15.0, 4.8, and 1.45 GHz and are plotted as filled diamonds in Figure 7. The residual flux densities (observed total flux densities minus the model wind values) are plotted as plus symbols in Figure 7. The residuals are primarily due to WR 147N, although a small fraction may be produced by the bridge between the two components.

WR 147N has an almost flat spectral index between 1.45 and 4.8 GHz, but it is definitely negative between 4.8 and 15.0 GHz. Since this component is presumably embedded in the wind of WR 147S at a distance of 364 AU, we must estimate the optical depths of the wind at this distance in order to determine its intrinsic spectrum. Using the expression for the *maximum* optical depth of a spherical wind with $\rho(r) \propto r^{-2}$ from Wright & Barlow (1975, eq. [5a]), we find *maximum* optical depths of 0.140 at 1.45 GHz, 0.011 at 4.80 GHz, and 0.001 at 15 GHz for a mass loss rate of $4.2 \times 10^{-5}\ M_\odot\ \mathrm{yr}^{-1}$, a wind terminal velocity of 900 km s^{-1}, an impact parameter of 364 AU, and a mean atomic weight per ion of 2.70. The actual optical depths are probably about half the above values. The maximum optical depths are too small to significantly alter the observed flux densities; even at 1.45 GHz, attenuation by the wind is less than 13%. We therefore conclude that the observed spectrum of WR 147N is about the same as its intrinsic spectrum.

4.3. *X-Ray Emission via Interaction of WR 147S with WR 147N*

The spectrum of WR 147N does not behave like a free-free stellar wind or an ultracompact H II region. It is also highly unlikely that it is a distant supernova almost aligned, by chance, with WR 147S, because an angular diameter $\leq 0\farcs1$, even at a distance of 15 kpc, would require the supernova to be less than 2 yr old. The existence of a radio bridge connecting the two sources strongly argues against a chance alignment with WR 147S. This leads us to consider possible scenarios in which the two radio sources are members of a binary star system, one of which is WR 147S with its associated strong thermal wind and the other is the nonthermal radio emitter WR 147N. At a distance of 630 pc, a separation of $0\farcs58$ corresponds to a projected separation of about 364 AU; the true separation could be larger, depending on the orbital inclination.

4.3.1. *Capture of a Spherical, Radiatively Driven Wind by a Neutron Star Companion*

In principle, one might expect that the object responsible for the nonthermal radio emission might also be responsible for the observed X-ray emission. If WR 147N were a collapsed object, such as a neutron star, which gravitationally captures stellar wind particles, it certainly would produce X-ray emission, although how it would produce nonthermal radio emission is not established. For a spherical wind with terminal velocity $v_\infty = 900$ km s^{-1} and $\dot{M} = 4.2 \times 10^{-5}\ M_\odot\ \mathrm{yr}^{-1}$, the wind density and mass flux at 364 AU from WR 147S would be $\rho_w(364\ \mathrm{AU}) \sim 7.9 \times 10^{-20}$ g cm^{-3} (equivalent to $\sim 1.8 \times 10^4$ ions cm^{-3}) and $F_m \sim 7.1 \times 10^{-12}$ g cm^{-2} s^{-1}, respectively. The mass flux is essentially independent of the orbital velocity of the secondary (i.e., WR 147N) since the orbital velocity is small relative to the wind velocity at a separation of 364 AU. We are assuming that WR 147N is at its projected distance from WR 147S; statistically, it is probably $\sim(2)^{1/2}$ larger. Let us assume that a neutron star of mass $M_n = 2\ M_\odot$ and radius $R_n = 15$ km is in orbit about WR 147S at a distance of 364 AU (the minimum separation). We will assume that the gravitational capture radius of the neutron star for stellar wind particles of velocity $v_\infty = 900$ km s^{-1} is given by

$$R_g = \frac{2GM_n}{v_\infty^2} \sim 6.6 \times 10^{10}\ \mathrm{cm}\ .$$

An accretion disk around the neutron star could increase the cross section beyond that given by R_g, but this seems unlikely in the environment considered here and we neglect this possibility. If all the gravitational potential energy of the captured wind particles were converted to X-ray emission, then the X-ray luminosity would be

$$L_x = \frac{GM_n \pi R_g^2 F_m}{R_n} = \frac{4\pi G^3 M_n^3 F_m}{R_n v_\infty^4} \sim 4.3 \times 10^{-3}\ L_\odot .$$

Thus, gravitational capture of wind particles by a neutron star fails by more than an order of magnitude to account for the observed X-ray luminosity ($\sim 0.13\ L_\odot$). If the wind speed were lower by a factor ~ 0.4 with the same mass loss rate, or if the capture radius were larger by about a factor of ~ 5.5 this mechanism could produce the observed X-ray luminosity, but it would have to convert gravitational energy to soft X-ray emission with 100% efficiency. The lower wind speed, however, would be in conflict with the observed He I 2.058 μm line.

Neutron stars have very strong surface magnetic fields (typically, $B_n \sim 10^{12}$ G). A fast stellar wind colliding with the magnetosphere of a neutron star would produce X-ray emission. The radius of the magnetosphere R_m of the neutron star should be about the distance at which the magnetic pressure is

balanced by the wind pressure:

$$R_m = \left[\frac{B_n^2 R_n^6}{8\pi\rho_w(r)v_\infty^2}\right]^{1/6} \sim 3.0 \times 10^{10} \text{ cm} .$$

This is only about half the gravitational capture radius. We, therefore, conclude that the collision of a spherical wind from WR 147S with the magnetosphere of a neutron star companion 364 AU distant cannot produce the observed X-ray luminosity.

4.3.2. *Collision of a Spherical Wind with the Magnetosphere of a B5 V Companion*

Let us assume that a B5 V companion is in orbit at a distance of 364 AU from WR 147S. We choose a B5 V star because it could be safely hidden from the speckle interferometry of Lortet et al. (1987). Using standard parameters from Allen (1973, p. 209) for a B5 V star and assuming a surface magnetic field of 20 G, we find a magnetospheric radius $R_m \sim 1.5 \times 10^{12}$ cm and an X-ray luminosity of

$$L_x = \tfrac{1}{2}\pi R_m^2 \rho_w(364 \text{ AU}) v_\infty^3 \sim 5.1 \times 10^{-5} L_\odot .$$

If all wind particles intercepted by the magnetosphere are captured and ultimately fall onto the surface of the B5 V star with conversion of all their gravitational potential energy into X-ray emission, the X-ray luminosity would only be $\sim 4.3 \times 10^{-5}$ $L_\odot$. Thus a hot massive companion does not appear to be capable of producing the observed X-ray luminosity by interacting with the wind from WR 147S.

4.3.3. *Capture of a Dense, Equatorial Wind by a Neutron Star Companion*

Here, we will return to the magnetic rotator model suggested for Be stars by Waters et al. (1988) and Poe et al. (1989) for W-R stars. We will investigate whether gravitational capture of a slow, dense, equatorial wind (driven by magnetic and rotational forces) from WR 147S by a 2 $M_\odot$ neutron star orbiting in the equatorial plane at a distance $r = 364$ AU can produce the observed X-ray luminosity. We will assume that WR 147S is viewed essentially pole-on; thus the He I 2.058 μm line gives the terminal velocity of its polar wind. If the half-opening angle of the equatorial disk is $\theta = 5°$ and the terminal velocity of the equatorial wind is $v_e = v_\infty/3 = 300$ km s^{-1}, where v_∞ is the terminal velocity of the polar wind, then the mass flux at WR 147N will be

$$F_m(r) = \rho_e(r)v_e = \frac{\dot{M}(v_\infty)}{4\pi r^2 \sin(\theta)} \frac{v_e}{v_\infty} \sim 2.7 \times 10^{-11} \text{ g cm}^{-2} \text{ s}^{-1} ,$$

where $\dot{M}(v_\infty) = 4.2 \times 10^{-5}$ $M_\odot$ yr^{-1}, $\rho_e(r)$ is the equatorial wind density at distance r, $\sin(\theta)$ is the fraction of the surface area of a sphere intercepted by a disk with half-opening angle θ, and $r = 364$ AU. The assumptions of 5° for θ and $v_\infty/3$ for v_e are arbitrary. θ was chosen to be small enough to significantly increase the mass flux in the equatorial wind over the spherical wind model. As will become apparent below, a reasonably large range of values for θ and v_e will easily satisfy the X-ray luminosity requirements, so our assumed values are not strongly restrictive for this model. The gravitational capture radius, in this case, is

$$R_g(v_e) = \frac{2GM_n}{v_e^2} \sim 2.6 \times 10^{11} \text{ cm} ,$$

and the maximum X-ray luminosity that could be produced by gravitational capture of equatorial wind particles is

$$L_x = \frac{GM_n}{R_n} \pi R_g(v_e)^2 F_m(r) \sim 1.3 \, L_\odot .$$

In this model, if only 10% of the gravitational potential energy of each captured particle were converted to soft X-ray emission, this mechanism could produce the observed soft X-ray luminosity. If v_e were increased to $v_\infty/2 = 450$ km s^{-1}, the maximum X-ray luminosity would be ~ 0.4 $L_\odot$, which is still large enough to produce the observed X-ray luminosity with $\sim 30\%$ conversion of gravitational potential energy to soft X-rays. If $\theta = 10°$ and $v_e = v_\infty/3$, then $L_x(\text{max}) \sim 0.7$ $L_\odot$. Since $L_x \propto v_e^{-3}$, one can see that a smaller value for v_e in the equatorial wind relative to that in a radiatively driven polar flow makes a substantial difference in the inferred X-ray luminosity. We conclude that this model can produce the observed X-ray luminosity for a reasonable range of values for θ and v_e. It only works, however, if v_e is significantly smaller than v_∞; in this case $v_e \leq 0.6 v_\infty$. A precise value will depend on the inclination of the equatorial disk to the line of sight, the value of θ, and the efficiency of converting gravitational potential energy to soft X-ray emission.

The collision of a slow, dense, equatorial wind with the magnetospheres of either a neutron star or a B5 V (or hotter) star at a distance of 364 AU fails by several orders of magnitude to produce the observed X-ray luminosity. A 1 $M_\odot$ white dwarf also does not have a deep enough gravitational potential well to produce the required X-ray luminosity by at least two orders of magnitude. Thus, of all the mechanisms we have investigated involving the interaction of a wind from WR 147S with WR 147N, the only one that can produce the observed X-ray luminosity is gravitational capture of a slow, dense, equatorial wind by a neutron star.

Of course, all the discussion above has been predicated on the assumption that the X-ray luminosity is produced in the nonthermal radio source WR 147N, which is assumed to be gravitationally bound to WR 147S. The X-ray emission, however, could be produced in the wind of WR 147S; an X-ray luminosity of $\sim 10^{-7}$ L_{bol} (~ 0.05 $L_\odot$ for WR 147S) is typical for W-R stars (Pollock 1987b). Pollock (1987b) has found that the average X-ray luminosity for single WN stars is $0.06 \pm 0.04 L_\odot$ and for WN binaries it is 0.13 ± 0.03 $L_\odot$. This suggests that on average about half of the X-ray luminosity in WN binaries is produced external to the WN star and its wind. Perhaps in the WR 147 system $\sim 50\%$ of the X-ray emission is produced in the wind of WR 147S and $\sim 50\%$ is produced external to WR 147S, possibly by wind interactions between WR 147S and WR 147N. The radio morphology and spectral indices of WR 147 is not suggestive of colliding winds similar to those in the MWC 349 system (Cohen et al. 1985) or HD 165052 (Luo, McCray, & Mac Low 1990; hereafter LMM), but they probably cannot be entirely ruled out from presently available data. If the wind from WR 147S dominates that from WR 147N, similar to that proposed for V444 Cyg by LMM, the scaling relation given by LMM indicates that this model produces far too little X-ray emission because of the large separation of WR 147S and WR 147N. It, therefore, appears unlikely that the X-ray emission is produced entirely in the wind of WR 147S or entirely in colliding winds between WR 147S and WR 147N. More likely is the scenario in which $\sim 50\%$ of the X-ray emission is produced in the wind of WR 147S and $\sim 50\%$ is produced exterior to WR

1475 perhaps by gravitational capture of a slow equatorial wind from WR 147 by a neutron star companion.

5. SUMMARY AND CONCLUSIONS

New near-infrared photometry is reported, which has resulted in a revised distance to WR 147 of 630 pc. This distance estimate is almost independent of reddening but it does depend on the assumption that WR 147 and WR 105 (both WN8 stars) have identical absolute magnitudes. WR 147 is *not* associated with the Cyg OB2 association (2 kpc away) as previously thought. A 2 μm spectrum of the star is presented which shows that the He I (2^1S–2^1P) line at 2.058 μm has a P Cygni profile whose blue absorption edge implies a terminal wind velocity of 900 km s^{-1} for WR 147S. It is suggested that this is probably the terminal velocity of the polar wind if the magnetic rotator model applies.

We have reported high-resolution VLA images of WR 147 at three different epochs. Observations were made at wavelengths 20, 6, 2, and 1.3 cm (although not all wavelength bands were imaged at each epoch) with angular resolutions of 1".60, 0".46, 0".14, and 0".11, respectively. These images confirm the results of Moran et al. (1989) that WR 147 is composed of two radio components separated by $\sim$0".6. The southern component is consistent with free-free emission from a wind but the northern component is clearly nonthermal. Theories which assume that the nonthermal emission is produced in the same star as the thermal wind are not applicable to WR 147. It was shown that the wind from WR 147 at a distance of 364 AU is essentially transparent at all frequencies greater than 1.4 GHz; thus, the observed radio spectrum is essentially the same as the intrinsic spectrum of the nonthermal component.

The radio emission from WR 147S, which is coincident with the optical WN8 star, can be accurately modeled by a spherical wind whose density decreases with distance as r^{-2}. Using our measured terminal wind velocity of 900 km s^{-1}, we find an average spherical mass loss rate of $4.2 \pm 0.2 \times 10^{-5}\ M_\odot$ yr^{-1} and a mean wind temperature of 9400 ± 1000 K. If the magnetic rotator model is adopted, the equatorial mass loss rate will be reduced relative to that from a spherical wind with terminal velocity v_∞ by the factor v_e/v_∞, where v_e is the equatorial wind speed.

Several mechanisms were considered to produce the observed X-ray luminosity by intercepting the wind from WR 147S by the nonthermal radio source WR 147N. The only mechanism we found that could produce adequate X-ray emission was gravitational capture by a neutron star orbiting WR 147S in a dense, slow, equatorial wind, as proposed in the magnetic rotator model of Poe et al. (1989). However, we also point out that the observed X-ray luminosity could be produced by shocks in the wind of WR 147S or possibly by colliding winds from WR 147S and WR 147N rather than in WR 147N as assumed. The colliding wind hypothesis does not appear promising for the WR 147 system based on its radio morphology and inferred energetics. A more likely scenario, based on the results of Pollock (1987b), is that $\sim$50% of the X-ray emission from WR 147 is produced in the wind of WR 147S and the remainder exterior to WR 147S perhaps by gravitational capture of wind particles from WR 147S by a companion neutron star.

WR 147 has been monitored at 21 and 6 cm with the WSRT during the period 1988.5 to 1990.7. These data show that the WR 147 system varies by as much as 50% at 21 cm over a period of a week or so and as much as 20% at 6 cm over a period of several weeks. These periods are too short to be explicable by varying amounts of free-free extinction in the wind of WR 147S as WR 147N orbits it. With an apparent separation of $\sim$365 AU, the orbital period is likely to be greater than 10^3 yr, so variations on time scales of weeks cannot be associated with orbital motion. We, of course, cannot rule out the possibility that the northern nonthermal source is itself a binary with components separated by $\ll$180 AU; 180 AU is the maximum separation allowed by the angular diameter of the northern component. The fact that the 21 cm variations have a larger amplitude than at 6 cm suggests that the variations are associated with the nonthermal radio component. The intrinsic spectrum of the northern component must be essentially the same as the observed spectrum since the stellar wind in which it is embedded at a distance of 364 AU from the WR star is transparent at all frequencies $\geq$1.4 GHz.

To further constrain the range of possible models for this system (and perhaps other systems like it) more observations are required. In particular, a sensitive visible spectrum might reveal the nature of a companion star and possibly orbital motion. X-ray observations using *ROSAT* could determine if the X-ray emission varies on time scales of minutes to hours, thereby establishing the size scale of the X-ray source. Regular monitoring at 6 and 21 cm is needed to determine the nature and possible periodicity of the variability shown in Figure 5. A radio pulsar search toward WR 147N should be undertaken. Since WR 147N is not a point, the observed nonthermal emission is unlikely to be due to a pulsar alone, but this does not rule out the possibility that such an object could be present.

We thank the staffs and directors of both the VLA and the WSRT, without whose support the observations reported here would not have been possible. The Westerbork Synthesis Radio Telescope is operated by the Netherlands Foundation for Research in Astronomy with financial support from the Netherlands Organization for Scientific Research (NWO). The United Kingdom Infrared Telescope is operated by the Royal Observatory, Edinburgh for the UK Science and Engineering Research Council. We are grateful to Tom Geballe for taking the infrared spectrum under the aegis of the UKIRT Service Observing Program. We thank Joe Cassinelli and John Mathis who critically read the manuscript and gave useful suggestions. We are also indebted to Dr. Andrew R. Taylor who refereed this paper and raised good questions and made several important suggestions which have improved the paper and sharpened our thinking. E. B. C. acknowledges partial support from NSF grant AST-8605125.

REFERENCES

Abbott, D. C., Bieging, J. H., & Churchwell, E. 1984, ApJ, 280, 671
———. 1985, in Radio Stars, ed. R. M. Hjellming & D. M. Gibson (Dordrecht Reidel), 219
Abbott, D. C., Bieging, J. H., Churchwell, E., & Torres, A. V. 1986, ApJ, 303, 239
Allen, C. W. 1973, Astrophysical Quantities (London: Athlone)
Baars, J. W. M., Genzel, R., Pauliny-Toth, I. I. K., & Witzel, A. 1977, A&A, 61, 99
Baars, J. W. M., Van der Brugge, J. F., Casse, J. L., Hamaker, J. P., Sondaar, L. H., Visser, J. J., & Wellington, K. J. 1973, Proc. IEEE, 61, 1258
Barlow, M. J., Smith, L. J., & Willis, A. J. 1981, MNRAS, 196, 101
Becker, R. H., & White, R. L. 1985a, in Radio Stars, ed. R. M. Hjellming & D. M. Gibson (Dordrecht: Reidel), 139
———. 1985b, ApJ, 297, 649
Bieging, J. H., Abbott, D. C., & Churchwell, E. B. 1982, ApJ, 263, 207
———. 1989, ApJ, 340, 518

Bos, A., Raimond, E., & Van Someren Greve, H. W. 1981, A&A, 98, 251
Caillault, J. P., Chanan, G. A., Helfand, D. J., Patterson, J., Nousek, J. A., Takalo, L. O., Bothun, G. D., & Becker, R. H. 1985, Nature, 313, 376
Cassinelli, J. P. 1990, in Angular Momentum and Mass Loss for Hot Stars, ed. L. A. Willson & R. Stalio (Dordrecht: Kluwer), 135
———. 1991, in Wolf-Rayet Stars and Interrelations with Other Massive Stars in Galaxies, ed. K. A. van der Hucht & B. Hidayat (Dordrecht: Kluwer), 289
Chen, W., & White, R. L. 1991, ApJ, 366, 512
Cohen, M., Bieging, J. H., Dreher, J. W., & Welch, W. J. 1985, ApJ, 292, 249
Conti, P. S., & Massey, P. 1989, ApJ, 337, 251
Dickel, H. R., Habing, H. J., & Isaacman, R. 1980, ApJ, 238, L39
Felli, M., & Massi, M. 1991, in IAU Symp. No. 143, Wolf-Rayet Stars and Interrelations with Other Massive Stars in Galaxies, ed. K. A. van der Hucht & B. Hidayat (Dordrecht: Kluwer), 87
Felli, M., Massi, M., & Catarzi, M. 1992, ApJ, submitted
Felli, M., & Panagia, N. 1982, ApJ, 262, 650
Florkowski, D. R., & Gottesman, S. T. 1977, MNRAS, 179, 105
Hillier, D. J. 1985, AJ, 90, 1514
Hogg, D. E. 1982, in IAU Symp. 99, Wolf-Rayet Stars: Observations, Physics, and Evolution, ed. C. W. H. de Loore & A. J. Willis (Dordrecht: Reidel), 221
———. 1989, AJ, 98, 282
Lortet, M.-C., Blazit, A., Bomean, D., & Foy, R. 1987, A&A, 180, 111
Lundstrom, I., & Stenholm, B. 1984, A&AS, 58, 163
Luo, D., McCray, R., & MacLow, M.-M. 1990, ApJ, 362, 267 (LMM)
Massey, P. 1984, ApJ, 281, 789
Merrill, P. W., & Burwell, C. G. 1950, ApJ, 112, 72
Moran, J. P., Davis, R. J., Bode, M. F., Taylor, A. R., Spencer, R. E., Argue, A. N., Irwin, M. J., & Shanklin, J. D. 1989, Nature, 340, 449
Persi, P., Tapia, M., Rodriguez, L. F., Ferrari-Toniolo, M., & Roth, M. 1990, A&A, 240, 93
Poe, C. H., Friend, D. B., & Cassinelli, J. P. 1989, ApJ, 337, 888
Pollock, A. M. T. 1987a, A&A, 171, 135
———. 1987b, ApJ, 320, 283
Prinja, R. K., Barlow, M. J., & Howarth, I. D. 1990, ApJ, 361, 607
Reynolds, S. P. 1986, ApJ, 304, 713
Schmid-Burgk, J. 1982, A&A, 108, 169
Schmutz, W. 1990, in Intrinsic Properties of Hot Luminous Stars, ed. C. D. Garmany (ASP Conf. Ser., 7), 117
Seaquist, E. R. 1976, ApJ, 203, L35
Smith, L. F. 1968, MNRAS, 138, 109
Stickland, D. J., Lloyd, C., & Willis, A. J. 1985, A&A, 150, L9
van der Hucht, K. A., Conti, P. S., Lindstrom, I., & Stenholm, B. 1981, Space Sci. Rev., 28, No. 3
van der Hucht, K. A., Hidayat, B., Admiranto, A. G., Supelli, K. R., & Doom, C. 1988, A&A, 199, 217
van der Hucht, K. A., Jurriens, T. A., Olnon, F. M., Thé, P. S., Wesselius, P. R., & Williams, P. M. 1985, in Birth and Evolution of Stars and Stellar Systems, ed. W. Boland & H. van Woerden (Dordrecht: Reidel), 167
Waters, L. B. F. M., Taylor, A. R., van den Heuvel, E. P. J., Habets, G. M. H. J., & Persi, P. 1988, A&A, 198, 200
White, R. L. 1985, ApJ, 289, 698
Williams, P. M., & Eenens, P. R. J. 1989, MNRAS, 240, 445
Williams, P. M., van der Hucht, K. A., Pollock, A. M. T., Florkowski, D. R., van der Woerd, H., & Wamsteker, W. M. 1990, MNRAS, 243, 662
Willis, A. J. 1991, in IAU Symp. 143, Wolf-Rayet Stars and Interrelations with Other Massive Stars in Galaxies, ed. K. A. van der Hucht & B. Hidayat (Dordrecht: Kluwer), 265
Wright, A. E., & Barlow, M. J. 1975, Mon.Noy.R.A.S., 170, 41
Zickgraf, F. J., Wolf, B., Stahl, O., Leitherer, C., & Klare, G. 1985, A&A, 143, 421